Moroccan Journal of Chemistry
ISSN: 2351-812X
http://revues.imist.ma/?journal=morjchem&page=login
SiKine & al. / Mor. J. Chem. 6 N°2 (2018) 342-353

New Corrosion inhibition of mild steel by 7-bromopyrido[2,3-b]pyrazine-2,3(1H, 4H)-dithiol in 1M hydrochloric acid solution

M. Sikine[1], Y. Kandri Rodi[1], A. Elyoussfi[2], A. Dafali[2], Y. Ouzidan[1], A. Kandri Rodi[1], F. Ouazzani Chahdi[1], E.M.Essassi[3,4], A. Chetouani[2], B. Hammouti[2] and H. Elmsellem[2*]

[1]Laboratory of Applied Organic Chemistry, Faculty of Science and Technology, University Sidi Mohammed Ben Abdallah, Fez, Morocco.

[2]Laboratoire de chimie analytique appliquée, matériaux et environnement (LC2AME), Faculté des Sciences, B.P. 717, 60000 Oujda, Morocco.

[3]Laboratoire de Chimie Organique Hétérocyclique, URAC 21, Pôle de Compétences Pharmacochimie, Mohammed V University in Rabat, Faculté des Sciences, Av. Ibn Battouta, BP 1014 Rabat, Morocco.

[4]Moroccan Foundation for Advanced Science, Innovation and Research (MASCIR), Rabat Design Center, Rue Mohamed Al Jazouli, Madinat El Irfane, Rabat, Morocco.

** Corresponding author: : h.elmsellem@gmail.com*

Received 03 Jan 2018,
Revised 22 Feb 2018,
Accepted 27 Feb 2018

Abstract

The corrosion inhibition performance of synthesized inhibitor 7-bromopyrido[2,3-b]pyrazine-2,3(1H,4H)-dithiol (M_2) was investigated on mild steel corrosion in 1 HCl using gravimetric and electrochemical measurements. The studied inhibitor, M_2showed the maximum inhibition efficiency (E) of 91% at a concentration as low as 10^{-3}M. The potentiodynamic polarization studies showed that the studied inhibitor (M_2) act as mixed inhibitor. The results of EIS studies showed that in the presence of inhibitor M_2, transfert charge resistance increased and Cdl decreased due adsorption of inhibitor at the mild steel surface. The adsorption of inhibitor molecules on mild steel surface obeys the Langmuir adsorption isotherm. The results of the theoretical investigation and experimental studies well complimented each other.

Keywords: *Mild steel; Corrosion; 7-bromopyrido[2,3-b]pyrazine-2,3(1H,4H)-dithiol; Quantum chemical parameters; Electrochemical; DFT.*

1. Introduction

Generally a metal and its environment causing degradation of the material and its properties, this degradation causes a major problem; this leads to plant closures, wasting precious resources. It can even cause serious accidents and contribute to the pollution of the natural environment, to reduce the impact of corrosion, may uses organic inhibitors, the toxicity of these compounds is decided about their harmful environmental characteristics[1,2].Heterocyclic compound chemistry is a very important extension, it occupies a predominant place in industry and pharmaceuticals, for example pyrido[2,3-b]pyrazine are prescribed for their properties anticancer[3],antitumor [4,5], antimalarial [6],anti-inflammatory [7],antibacterial effects [8] . Most organic compounds contain heteroatoms such that N, O, P and S [9, 10] are considered as active centers capable of discharging the electrons with the surface of the metal they have a good inhibitory efficiency. [11, 12, 13]They can also pyrido[2,3-b]pyrazine derivatives has a good inhibitory action on the corrosion of metals.[14,15] The aim of the presents study is to evaluate the corrosion inhibition efficiency of mild steel in hydrochloric acid solution by 7-bromopyrido[2,3-b]pyrazine-2,3(1H,4H)-dithiol ,The title compound (M_2) was obtained in good yield, produced by condensation 7-bromo-pyrido[2,3-b]pyrazine-2,3(1H,4H)dione with phosphorus pentasulfide in pyridine the structure of the product is determined by spectroscopic and elemental analysis. In the present study, by7-bromopyrido[2,3-b]pyrazine-2,3(1H,4H)-dithiol has been investigated for its corrosion inhibition efficiency. Weight loss studies, polarization (Tafel) studies and impedance studies were employed to investigate the inhibition efficiency of by7-bromopyrido[2,3-b]pyrazine-2,3(1H,4H)-dithiol on MS in acidic chloride solution. The results of quantum chemical methods were correlated with experimental results.Figure 1.

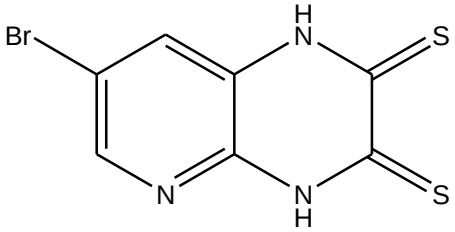

Figure 1. Chemical structure of 7-bromopyrido[2,3-b]pyrazine-2,3(1H,4H)-dithiol (M_2).

2. Experimental

2.1. Synthesis of inhibitor

The 7-bromopyrido[2,3-b]pyrazine-2,3(1H,4H)-dithiol was synthesized by the condensation of (1g; 4.13 mmol) 7-bromo-pyrido[2,3-b]pyrazine-2,3(1H,4H)dione with (2.75g; 12.39mmol) phosphorus pentasulfide in 30 ml of pyridine. The mixture reaction is refluxed for 7 hours, after evaporation of pyridine the residue was washed with hot water and then filtered .The compound was obtained in 82%(Scheme1).

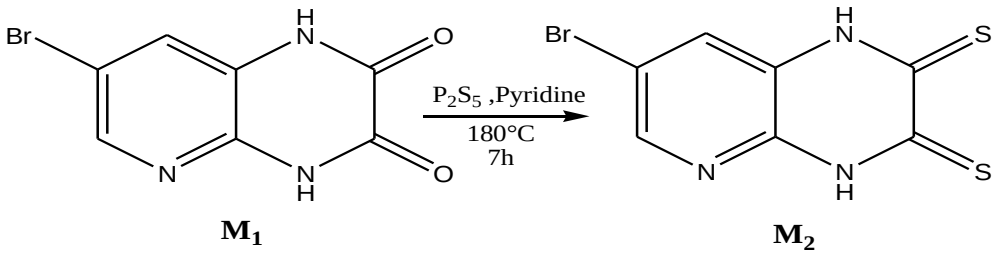

Scheme 1. Synthesis of 7-bromopyrido[2,3-b]pyrazine-2,3(1H,4H)-dithiol (M_2).

The analytical and spectroscopic data are conforming by ^{1}H, ^{13}C NMR spectra and IR.

(M_2): Yield = 82%; **Melting point**> 300°C; **^{1}H NMR (DMSO-d_6) δ ppm:** 14.29 (S, 1H, NH); 14.71 (S, 1H, NH); 7.82 (d, 1H, CHpyr, J= 2.1 Hz); 8.37(d, 1H, CHpyr).**^{13}C NMR (DMSO-d_6) δ ppm:** 180.11; 181.82 (2N-C=S); 124.87; 139.69 (Cq); 125.15; 145.26 (CH_{pyr}).

IR (KBr)cm^{-1}: 1446.35.

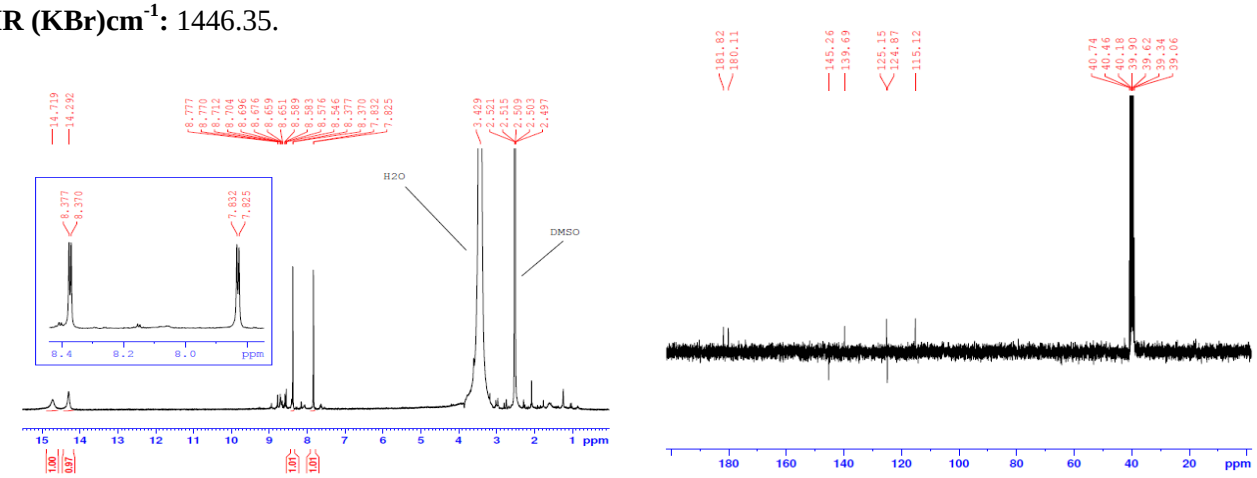

Figure 2.^{1}H NMR; ^{13}CNMR spectrum of M2

2.2. Materials and solutions

2.2.1. Materials and test solution

The mild steel specimens having chemical composition (wt %) C 0.076%, Si 0.026%, Mn 0.192, P 0.012%, Cr 0.050%, Ni 0.050%, Al 0.023% and Cu 0.135% and Fe 99.30% were used for gravimetric and electrochemical experiments. The specimens with dimension 1.5 cm × 1.5 cm × 0.05 cm were used for gravimetric test. The mild steel specimens were abraded by SiC abrasive papers (from grade 600 to 1200), rinsed with distilled water, degreased in acetone. The test solution of 1M HCl was prepared by the dilution of analytical grade hydrochloric acid (HCl, 37 %, Fisher Scientific) with double distilled water.

2.2.2. Polarization Measurements

The electrochemical study was carried out using a potentiostat PGZ100 piloted by Voltamastersoft-ware. This potentiostatis connected to a cell with three electrode thermostats with double wall. A saturated calomel electrode (SCE) and platinum electrode were used as reference and auxiliary electrodes, respectively. Anodic and cathodic potentiodynamic polarization curves were plotted at a polarization scan rate of 0.5mV/s. Before all experiments, the potential was stabilized at free potential during 30 min. The polarisation curves are obtained from −800 mV to −200 mV at 308 K. The solution test is there after de-aerated by bubbling nitrogen.

2.2.3. Impedance measurements

The electrochemical impedance spectroscopy (EIS) measurements are carried out with the electrochemical system, which included a digital potentiostat model Voltalab PGZ100 computer at Ecorr after immersion in solution without bubbling. After the determination of steady-state current at a corrosion potential, sine wave voltage (10 mV) peak to peak, at frequencies between 100 kHz and 10 mHz are superimposed on the rest potential. Computer programs

automatically controlled the measurements performed at rest potentials after 0.5 hour of exposure at 308 K. The impedance diagrams are given in the Nyquist representation. Inhibition efficiency (EEIS %) is estimated using the relation (1), [16].

E_{EIS} % = ($R_{ct} - R^{\circ}_{ct} / R_{ct}$) x 100 **(1)**

Where, R°ct and Rct are the charge transfer resistance values in the absence and presence of inhibitor, respectively:

3. Results and discussion

3.1. Weight loss measurement

In order to give an initial insight into the inhibitive effect of by7-bromopyrido[2,3-b]pyrazine-2,3(1H,4H)-dithiol (M_2), the weight loss measurements method which is very easy and inexpensive was used due to its good reliability. The values of the ηW(%), and corrosion rates (W) calculated from gravimetric measurements are listed in Table 1. The following equations were used to calculate the inhibition efficiency ηW(%) and the surface coverage (θ) [17]:

E_w(%)=[1-w/w°]x100 **(2)**

Where W° and W are the corrosion rates without and with various concentrations of the by 7-bromopyrido[2,3-b]pyrazine-2,3(1H,4H)-dithiol(M_2), respectively, θ is the degree of surface coverage of tested inhibitor(M_2). The data in Table 1 clearly indicates that, regardless of used concentration, the addition of by7-bromopyrido[2,3-b]pyrazine-2,3(1H,4H)-dithiol (M_2) to corrosive medium yield a considerable decrease of the corrosion rate. At this point, it is worth mentioning that the obtained results demonstrate high corrosive activity of tested inhibitor (M_2) which in most cases is usually due to its adsorption on mild steel surface, reducing the surface area available for the HCl attack through an effective blockage of active sites. The inhibition mechanisms of tested inhibitor for the steel corrosion were further studied by means of electrochemical methods.

Table1. Corrosion rate and inhibition efficiency in the absence and presence of M_2 in 1.0 M HCl solution.

Inhibitor	**C** (mol/l)	**w** ($mg.cm^{-2} h^{-1}$)	**E_w** (%)	**θ**
1M HCl	--	0.82	--	--
M_2	**10^{-6}**	0.35	57	0.57
	10^{-5}	0.27	67	0.67
	10^{-4}	0.15	82	0.82
	10^{-3}	0.07	**91**	0.91

3.2. Adsorption isotherm and thermodynamic parameters

The adsorption of inhibitor molecules is one of the most important topics in corrosion researches. Its importance comes from not only due to its ability to provide structural information of the double layer but also due to the thermodynamic information can provide. In general, the adsorption of organic molecules on the electrode surface can be classified into two categories. First, the molecules adsorb but retain their chemical individuality. The adsorption bond between molecule and surface is relatively weak and molecules may exchange readily their peer molecules from solution. This is a reversible type of adsorption. In contrast, the interaction between molecule and surface may be very

strong. This may result in a charge transfer between them, therefore new species mayform. This is the irreversible type adsorption [18]. In this study, in order to identify the nature and the strength of adsorption a series of experimental adsorption isotherms were obtained is seen in Figure3, and the best fit was determined with the use of the Langmuir adsorption isotherm. It is represented by the following equation [19]:

$$\frac{C}{\theta} = \frac{1}{K} + C \quad \textbf{(3)}$$

Where C is the concentration of inhibitor, K the adsorption equilibrium constant, and θ is the surface coverage values for various concentrations of the inhibitor M_2 in acidic solution; it has been evaluated from the gravimetric measurement. The K_{ads} is the adsorption equilibrium constant, which is 1.71 10^5reflects more efficient adsorption hence better inhibition efficiency of M_2 on the mild steel surface [20, 21]. The equilibrium constant for the adsorption–desorption process is related to the standard free energy of adsorption ΔG_{ads} according to relation [22]:

$$\Delta G_{ads} = -RT \ln(55.5K) \quad \textbf{(4)}$$

Where R is the universal gas constant and T is the absolute temperature; the calculated ΔG_{ads} was _38.97 kJ mol^{-1}. The values of ΔG_{ads} around 20 kJ mol_1 or lower are indicates that the electrostatic interaction between inhibitor and the electrode surface (physisorption); those around 40 kJ mol_1 or higher involve charge sharing or transfer from the inhibitor to the metal surface to form a coordinate type of bond (chemisorption) [23–24]. The value of ΔG_{ads} for M_2 was lower than 40 kJ mol^{-1} but closer to 40 kJ mol^{-1} which showed that physical adsorption.

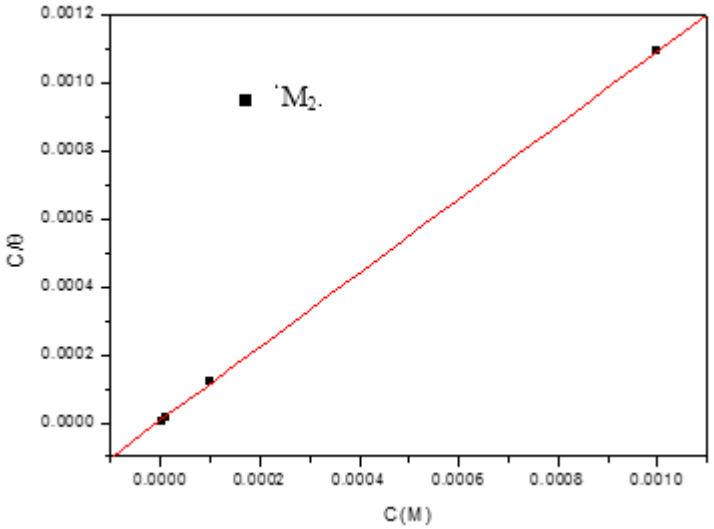

Figure 3. Langmuir adsorption plot for the mild steel electrode in 1 M HCl containing different concentrations of M_2.

3.2. Electrochemical Measurements

The electrochemical measurements were carried out using Volta lab (Tacussel - Radiometer PGZ 100) potentiostat controlled by Tacussel corrosion analysis software model (Voltamaster 4) at static condition. The corrosion cell used had three electrodes. The reference electrode was a saturated calomel electrode (SCE). A platinum electrode was used as auxiliary electrode of surface area of 1 cm^2. The working electrode was carbon steel of the surface 1cm^2. All potentials given in this study were referred to this reference electrode. The working electrode was immersed in the test solution for 30 minutes to establish a steady state open circuit potential (E_{ocp}). After measuring the E_{ocp}, the electrochemical measurements wereperformed. All electrochemical tests have been performed in aerated solutions at 308 K. The EIS experiments were conducted in the frequency range with high limit of 100 kHz and different low limit 0.1 Hz at open circuit potential, with 10 points per decade, at the rest potential, after 30 min of acid immersion, by

applying 10 mV ac voltage peak-to-peak. Nyquist plots were made from these experiments. The best semicircle can be fit through the data points in the Nyquist plot using a non-linear least square fit so as to give the intersections with the x-axis.

3.2.1. Tafel plots measurements

Tafel curves in without and with various concentration of M_2 at 308 K were performed (Figure 4). The Tafel polarization parameters, including, corrosion current density (i_{corr}), corrosion potential (E_{corr}), anodic (βa) and cathodic (βc) Tafel slopes are all summarized in Table 2. In the case of polarisation method the relation determines the inhibition efficiency (EI%), where $I°_{corr}$ and I_{corr} are the uninhibited and inhibited corrosion current densities [25]:

$$E_I\% = (1 - \frac{I_{corr}}{I^{\circ}_{corr}}) \times 100 \quad \textbf{(5)}$$

The inspection of Figure 4 reveals apparent displacement of cathodic and anodic current densities upon increasing the concentration of the M_2. The presence of M_2 causes significant decrease in the anodic and cathodic branches with no defi- nite change in the corrosion potential Ecorr suggesting that M_2 behaves as mixed type inhibitor [26]. Upon inspection of Figure4, is clear that the cathodic branches of the polarisation curves of the mild steel in uninhibited and inhibited solution are giving rise to parallel Tafel lines which indicates that the mechanism of corrosion reaction with and without M_2 is the same and that the charge transfer mechanism controls the hydrogen evolution as well as the reduction of H^+ ions. In the anodic branches, it can be seen that the addition of the tested inhibitor M_2 to corrosive solution reduces the metal dissolution rate compared to the HCl solution. On the other hand, the results in Table 2 also show significant decrease in the value of icorr with increasing M_2 concentration. These effects on current densities can be explained by the fact that the addition of the inhibitor M_2 reduces considerably the hydrogen evolution and the dissolution of M_2 at cathodic and anodic reactions, respectively. On increasing M_2 concentration, the E% increases and reached a maximum of 89% at 10^{-3}M.

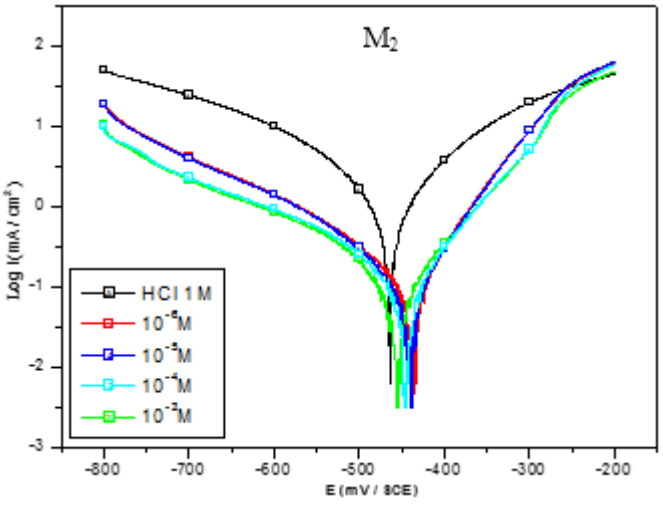

Figure 4: Tafel plot of mild steel with different concentrations of M_2 in 1M HCl solution.

Table 2: Tafel polarization parameters obtained at different concentrations of M_2.

Inhibitor	Concentration (M)	- E_{corr}(mV/SCE)	I_{corr} (µA/cm^2)	$-\beta_c$ (µA/cm²)	E_I (%)
HCl	1	464	1386	164	--
M_2	10^{-6}	452	379	121	73
	10^{-5}	447	291	153	79
	10^{-4}	444	217	169	84
	10^{-3}	449	156	173	89

3.2.2. Electrochemical impedance spectroscopy (EIS)

Electrochemical impedance spectroscopy (EIS) is commonly used technique in corrosion researches to explain the mechanisms and adsorption phenomena [27, 28]. Especially, in inhibition studies, a single semi-circular shape is observed for mild steel in HCl [29, 30]. As the concentration of by7-bromopyrido[2,3-b]pyrazine-2,3(1H,4H)-dithiolM_2 increases, the diameter of Nyquist semicircles(Figure 5) also showed higher resistance transfert that was generally larger than that of the uninhibited system. This suggests the increases in the growth inhibitive effect of by7-bromopyrido[2,3-b]pyrazine-2,3(1H,4H)-dithiolM_2 through its adsorption on mild steel surface.

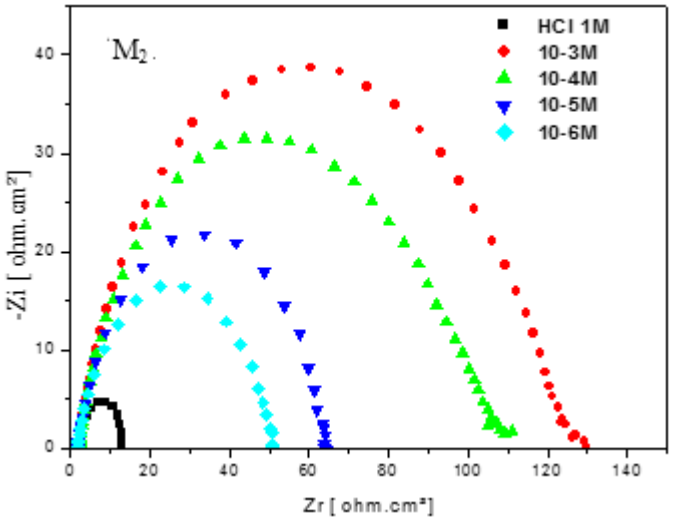

Figure 5. Electrochemical impedance spectra (Nyquist plots) of MS in 1.0 M HCl solution without and with different concentrations of M_2 at 308 K.

In Table 3 there is a clear trend of increasing polarization resistance values accompanied with significant decrease in the double layer capacitance over increasing concentrations of by7-bromopyrido[2,3-b]pyrazine-2,3(1H,4H)-dithiolM_2, meaning the effective adsorption of larger M_2 molecules on the MS surface. The decrease in the C_{dl} values at higher concentration may be due to a decrease in dielectric constant, hence an increased ability to adsorption of tested inhibitor resulting the better protection of metal (MS) against dissolution [31]. As confirmation, we note from Table 3 that the values of the inhibition efficiency were increased markedly and reached 91% at 10^{-3}M. In Figure5, Nyquist plots for mild steel in 1 M HCl solution with, and without different concentrations of the by7-bromopyrido[2,3-b]pyrazine-2,3(1H,4H)-dithiolM_2 were seen. The Rct increased with increasing M_2 concentration.

The maximum value was 129(Ω cm^2) in Table 3. Thus, the results obtained from EIS, electrochemical techniques and gravimetric study arealso in good agreement.

Table 3: Impedance parameters for MS corrosion in 1.0 M HCl solution without and with differentconcentrations of M_2 at 308 K.

Inhibitor	Conc(M)	R_{ct}(Ω cm^2)	C_{dl}(μFcm^{-2})	θ	E_{EIS}%
1.0 M HCl	--	10	200	--	--
M_2	10^{-6}	51	104	0.76	76
	10^{-5}	65	93	0.82	82
	10^{-4}	106	71	0.89	89
	10^{-3}	129	65	0.91	**91**

3.3. Theory and computational details

Quantum chemical calculations are used to correlate experimental data for inhibitors obtained from different techniques (viz., electrochemical and weight loss) and their structural and electronic properties. According to Koop man's theorem [32], E_{HOMO} and E_{LUMO} of the inhibitor molecule are related to the ionization potential (I) and the electron affinity (A), respectively. The ionization potential and the electron affinity are defined as $I = -E_{HOMO}$ and $A = -E_{LUMO}$, respectively. Then absolute electronegativity (χ) and global hardness (η) of the inhibitor molecule are approximated as follows [33]:

$$\chi = \frac{I+A}{2}\ ,\quad \chi = -\frac{1}{2}(E_{HOMO} + E_{LUMO}) \quad \textbf{(6)}$$

$$\eta = \frac{I-A}{2}\ ,\quad \eta = -\frac{1}{2}(E_{HOMO} - E_{LUMO}) \quad \textbf{(7)}$$

Where $I = -E_{HOMO}$ and $A = -E_{LUMO}$ are the ionization potential and electron affinity respectively.

The fraction of transferred electrons ΔN was calculated according to Pearson theory [34]. This parameter evaluates the electronic flow in a reaction of two systems with different electronegativities, in particular case; a metallic surface (Fe) and an inhibitor molecule. ΔN is given as follows:

$$\Delta N = \frac{\chi_{Fe} - \chi_{inh}}{2(\eta_{Fe} + \eta_{inh})} \quad \textbf{(8)}$$

Where χ_{Fe}andχ_{inh} denote the absolute electronegativity of an iron atom (Fe) and the inhibitor molecule, respectively; η_{Fe} and ηinh denote the absolute hardness ofFe atom and the inhibitor molecule, respectively. In order to apply the eq.4 in the present study, a theoretical value for the electronegativity of bulk iron was used χ_{Fe} = 7 eV and a global hardness of η_{Fe} = 0, by assuming that for a metallic bulk I = A because they are softer than the neutral metallic atoms [35]. The electrophilicityhas been introduced by Sastri and al. [36], is a descriptor of reactivity that allows a quantitative classification of the global electrophilic nature of a compound within a relative scale. They have proposed the ω as a measure of energy lowering owing to maximal electron flow between donor and acceptor and ω is defined as follows.

$$\omega = \frac{\chi^2}{2\eta} \quad \textbf{(9)}$$

The Softness σ is defined as the inverse of the η [36];

$$\sigma = \frac{1}{\eta} \quad \textbf{(10)}$$

Using left and right derivatives with respect to the number of electrons, electrophilic and nucleophilic Fukui functions for a site k in a molecule can be defined [36].

$$f_k^+ = P_k(N+1) - P_k(N) \quad for\ nucleophilic\ attack \quad \textbf{(11)}$$

$$f_k^- = P_k(N) - P_k(N-1) \quad for\ electrphilic\ attack \quad \textbf{(12)}$$

$$f_k^+ = [P_k(N+1) - P_k(N-1)]/2 \quad \text{for radical attack} \quad \textbf{(13)}$$

3.3.1. Quantum chemical calculations

The FMOs (HOMO and LUMO) are very important for describing chemical reactivity. The HOMO containing electrons, represents the ability (E_{HOMO}) to donate an electron, whereas, LUMO haven't not electrons, as an electron acceptor represents the ability (E_{LUMO}) to obtain an electron. The energy gap between HOMO and LUMO determines the kinetic stability, chemical reactivity, optical polarizability and chemical hardness–softness of a compound [37]. Firstly, in this paper, we calculated the HOMO and LUMO orbital energies by using B3LYP method with 6-31G(d,p). All other calculations were performed using the results with some assumptions. The higher values of E_{HOMO} indicate an increase for the electron donor and this means a better inhibitory activity with increasing adsorption of the inhibitor on a metal surface, where as E_{LUMO} indicates the ability to accept electron of the molecule. The adsorption ability of the inhibitor to the metal surface increases with increasing of E_{HOMO} and decreasing of E_{LUMO}. The HOMO and LUMO orbital energies and image of M_2 were performed and were shown in Table 5 and Figure6. High ionization (5.88 eV and 6.20 eV in gas and aqueous phases respectively) indicates high stability [38], the number of electrons transferred (ΔN) was also calculated and tabulated in Table 4. The $\Delta N < 3.6$ indicates the tendency of a molecule to donate electrons to the metal surface [39, 40].

Table 4. Quantum chemical descriptors of the studied inhibitor M_2 at B3LYP/6-31 G** in gas, G and aqueous, A phases and the inhibition efficiencies as given in [41, 42].

Inhibitor	Phase	TE (eV)	E_{HOMO} (eV)	E_{LUMO} (eV)	Gap ΔE (eV)	μ (D)	IP (eV)	EA (eV)	X (eV)	η (eV)	ω	σ	ΔN
M_2	**G**	-103430.6	-5.8899	-2.8788	3.0111	5.9706	5.8899	2.8788	4.3843	1.5055	2.8090	0.6642	0.8687
	A	-103431.1	-6.2033	-3.1194	3.0840	10.4011	6.2033	3.1194	4.6613	1.5420	7.0455	0.6485	0.7583

The final optimized geometries of M_2 in gas and aqueous, selected valence bond angle and dihedral angles and bond lengths are given in Figure6.

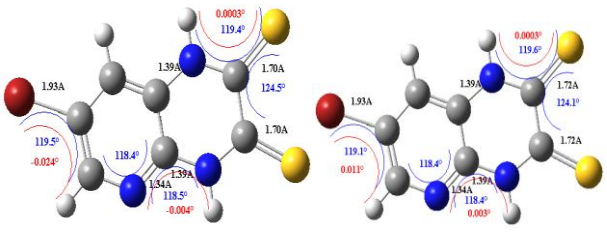

M_2Gas phase M_2 Aqueous phase

Figure 6. Optimized molecular structures, selected dihedral angles (red), valence bond angle (blue) and bond lengths (black) of the studied inhibitors calculated in gas and aqueous phases at B3LYP/6-31G(d,p) level ofM_2**.**

After the analysis of the theoretical results obtained, we can say that the molecule M_2 have a non-planar structure.

Table 5.The HOMO and the LUMO electrons density distributions of the studied inhibitor M_2 computed at B3LYP/6-31G (d,p) level in gas and aqueous phases.

	M_2Gas phase	M_2Aqueous phase
HOMO M_2	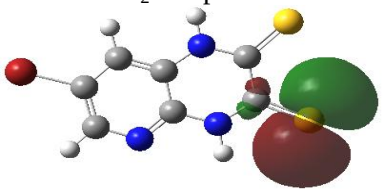	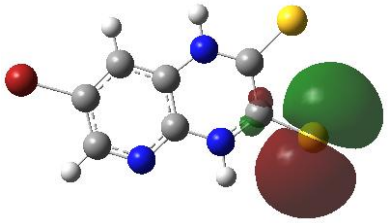
LUMO M_2	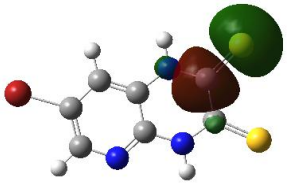	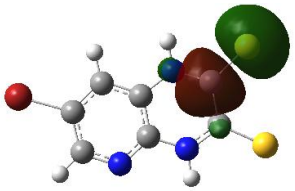

The inhibition efficiency afforded by the 7-bromopyrido[2,3-b]pyrazine-2,3(1H,4H)-dithiolM_2 may be attributed to the presence of electron rich N.

4. Conclusion

- The inhibition efficiencies of the inhibitor M_2 obtained from weight loss, potentiodynamic polarization and impedance methods are in good agreement.
- Potentiodynamic polarization studies have shown that M_2 derivatives act as mixed-type inhibitor, and their inhibition mechanism is adsorption.
- Data EIS measurements reveals that the studied M_2 inhibit MS corrosion by getting adsorbed at the MS/electrolyte interfaces there by forming the surface protective film which isolates the MS from the corrosive environment. The increased values of R_{ct} and decreased values of C_{dl} justify the observation.
- The adsorption of M_2 derivatives on the MS surface, in 1.0 M HCl solution wasfound to obey Langmuir's adsorption isotherm with a high negative value of the free energy of adsorption.
- DFT simulations technique incorporating molecular mechanics can be used to simulate the adsorption of M_2 derivatives on MS surface in 1.0 M HCl.

References

[1]B. Zerga, M. Sfaira, Z. Rais, M. Ebn Touhami, M. Taleb, B. Hammouti, B. Imelouane, A. Elbachiri, Matériaux & techniques, 97 (2009) 297.

[2]J. Sinko, Prog. Org. Coat. 42 (2001) 267.

[3]Orestis Argyros, Nikolaos Lougiakis, Eva Kouvari, Alexandra Papafotika, Catherine P. Raptopoulou, Vassilis Psycharis, Savvas Christoforidis, Nicole Pouli, Panagiotis Marakos, Constantin Tamvakopoulos. European Journal of Medicinal Chemistry, S0223-5234(16)31031-5. 10.1016/j.ejmech.2016.12.025

[4]I. Seipelt, S. Baasner, M. Gerlach, M. Teifel, J. Fensterle, L. Blumenstein, G.Mueller, E. Guenther, AEZS-126, a new orally bioavailable PI3K inhibitor in preclinical development, Cancer Res. 69 (2009) 3705-3705.

[5]I. Seipelt, E. Clasu, T. Schuster, E. Polymeropoulos, M. Teifel, E. Gunther, New generation of anilino-substituted pyridopyrazine-urea derivatives show highly selective PI3K-inhibition, Cancer Res. 67 (2007) 2379-2379.

[6]A. Chandra Shekhar , P. Shanthan Rao , B. Narsaiah , Aparna Devi Allanki ,Puran Singh Sijwali. European Journal of Medicinal Chemistry . 77(2014) 280-287

[7]Kevin J. Hodgetts , Charles A. Blum , Timothy Caldwell , Rajagopal Bakthavatchalam, Xiaozhang Zheng ,Scott Capitosti , James E. Krause , Daniel Cortright , Marci Crandall , Beth Ann Murphy , Susan Boyce ,A. Brian Jones , Bertrand L. Chenard. Bioorganic & Medicinal Chemistry Letters 20 (2010) 4359–4363

[8]M. Sikine, Y. Kandri Rodi, H. Misbahi, M. Chraibi, A. Kandri Rodi,F. Ouazzani Chahdi , K. Fikri Benbrahim and E.M.Essassi. J.MAR.CHIM.HETEROCYCL. 1 (16)(2017)119-123

[9]M. Sikine, Y. Kandri Rodi, H. Elmsellem, O. Krim, H. Steli, Y. Ouzidan, A. Kandri Rodi, F. Ouazzani Chahdi, N. K. Sebbar, E. M. Essassi. J. Mater. Environ. Sci. 7 (4) (2016)

(2016) 4620-4632

[11]Kaddouri M., Bouklah M., Rekkab S., Touzani R., Al-Deyab S.S., Hammouti B., Aouniti A., Kabouche Z., Int. J. Electrochem. Sci. 7(2012)9004–9023.

[12]Yurt A., Balaban A., Kandemir S.U., Bereket G., Erk B., Mater. Chem. Phys.

85(2004)420–426.

[13]Elmsellem H., Basbas N., Chetouani A., Aouniti A., Radi S., Messali M., Hammouti B., Portugaliae. *Electrochimica. Acta*. 2(2014)77.

[14]M. Y. Hjouji, M. Djedid, H. Elmsellem, Y. Kandri Rodi, Y. Ouzidan, F. Ouazzani Chahdi, N. K. Sebbar, E. M. Essassi, I. Abdel-Rahman, B. Hammouti. J. Mater. Environ. Sci. 7 (4) (2016) 1425-1435

[15]M. Y. Hjouji,M. Djedid, H. Elmsellem, Y. Kandri Rodi, M. Benalia, H. Steli ,Y. Ouzidan, F. Ouazzani Chahdi, E. M. Essassi and B. Hammouti. Der Pharma Chemica. 8(4) (2016)85-95.

[16] H. Elmsellem, T. Harit, A. Aouniti, F. Malek, A. Riahi, A. Chetouani, B. Hammouti, Protection of Metals and Physical Chemistry of Surfaces. 51 (2015) 873–884.

[17] H. Elmsellem , H.Nacer, F.Halaimia, A.Aouniti, I.Lakehal, A.Chetouani, ,Int. J. Electrochem. Sci, 9 (2014) 5328-5351.

[18] A. Aouniti, H. Elmsellem, S. Tighadouini, Journal of Taibah University for Science, (2015),

http://dx.doi.org/10.1016/j.jtusci.2015.11.008.

[19] H. Elmsellem, N. Basbas, A. Chetouani, A. Aouniti, Portugaliae. Electrochimica Acta, 2 (2014) 77-108.

[20] H. Elmsellem , M. H. Youssouf, A. Aouniti, Russian, Journal of Applied Chemistry. 8 (2014) 744−753.

[21] Y. El Ouadi, Lahhit, N., Bouyanzer, A. Elmsellem, H., Majidi, L., Znini, M., Abdel Rahman, I., Hammouti, B., El Mahi, B. and Costa, J. International Journal of Development Research,6 (2016) 6867-6874.

[22] H. Elmsellem, AounitiA., YoussoufiM.H., BendahaH., Ben hadda T., Chetouani A., Warad I., Hammouti B., Phys. Chem. News, 70 (2013) 84.

[23] H. Elmsellem, Elyoussfi A., Sebbar N. K., Dafali A., Cherrak K., Steli H., Essassi E. M., Aouniti A. and Hammouti B., Maghr. J. Pure & Appl. Sci, 1 (2015) 1-10.

[24] H. Elmsellem, Aouniti A.,Khoutoul M., Chetouani A., Hammouti B., Benchat N.,

Touzani R. and Elazzouzi M., J. Chem. Pharm. Res, 6 (2014) 1216.

[25] M. Sikine, H. Elmsellem, Y. Kandri Rodi, H. Steli, A. Aouniti, B. Hammouti, Y. Ouzidan, F. Ouazzani Chahdi, M. Bourass, and E. M. Essassi, J. Mater. Environ. Sci. 7 (2016) 4620-4632.

[26] S. Bourichi, Y. Kandri Rodi, H. Elmsellem, H. Steli, Y. Ouzidan, N. K. Sebbar, F. Ouazzani Chahdi, E. M. Essassi, F. El-Hajjaji and B. Hammouti, Der Pharma Chemica, 8 (2016) 179-186.

27. S. Lahmidi, H. Elmsellem, A. Elyoussfi, Sebbar N. K., Essassi E.M., Ouzidan Y., KandriRodi Y., DguiguiK., El Mahi B. and Hammouti B., *Der PharmaChemica*. 8(1) (2016) 294.

28. H. Bendaha, H. Elmsellem, A. Aouniti, M. Mimouni, Chetouani A., Hammouti B., *Physicochemical Mechanics of Materials.* 1 (2016) 111-118.

29. H. Elmsellem, A. Aouniti, M. Khoutoul, Chetouani A., Hammouti B., Benchat N., Touzani R. and Elazzouzi M., *J. Chem. Pharm. Res*. 6 (2014) 1216.

30. H. Elmsellem,K. Karrouchi, Aouniti A., Hammouti B., Radi S., Taoufik J., Ansar M., Dahmani M., H. Steli and El Mahi B., *Der PharmaChemica*. 7(10) (2015)237-245.

31. N. K. Sebbar, H. Elmsellem, M. Boudalia, lahmidi S., Belleaouchou A., Guenbour A., Essassi E. M., Steli H., Aouniti A., *J. Mater. Environ. Sci*. 6 (11) (2015) 3034-3044.

32. Pearson R.G., *Inorg. Chem*. 27 (1988) 734.

33. Sastri V.S., Perumareddi J.R., *Corrosion*. 53 (1997) 617.

34. H. Elmsellem, Nacer H., Halaimia F., Aouniti A., Lakehal I., Chetouani A., Al-Deyab S. S., Warad , R. Touzani, Hammouti B., *Int. J. Electrochem. Sci*. 9(2014)5328.

35. Z. Tribak , Y. KandriRod, H. Elmsellem, Abdel-Rahman I., Haoudi A., Skalli M. K., Kadmi Y., Hammouti B., Ali Shariati M., Essassi E. M., *J. Mater. Environ. Sci*. 8 (2017) 1116 -1127.

36. P. Udhayakala, Rajendiran T. V., Gunasekaran S., *Journal of Chemical, Biological and Physical Sciences A*, 2(3) (2012)1151–1165.

37. Govindarajan M., Karabacak M., *Spectrochim. Acta Part A MolBiomolSpectrosc*. 85(2012) 251.

38. A. L. Essaghouani, H. Elmsellem, M. Ellouz, El Hafi M., Boulhaoua M., Sebbar N. K.,Essassi E. M., M. Bouabdellaoui , Aouniti A. and Hammouti B., *Der PharmaChemica*. 8(2)(2016)297-305.

39. I. Lukovits, E. Kalman, F. Zucchi, *Corrosion*. 57 (2001) 3.

40. A. Elyoussfi, A. Dafali, H. Elmsellem, H. Steli, Y. Bouzian, K. Cherrak, Y. El Ouadi, A. Zarrouk,

B. Hammouti, *J. Mater. Environ. Sci.* 7 (9) (2016) 3344.

41. M. Ramdani, H. Elmsellem, N. Elkhiati, B. Haloui, A. Aouniti,M. Ramdani, Z. Ghazi,A. Chetouani and B. Hammouti, *Der pharma chem.*7 (2015) 67-76.

42. H. Darmokoesoemo, H.Setyawati, A. T .A. Ningtyas,Y. Kadmi, Heri Septya Kusuma. Results in Physics. http://dx.doi.org/10.1016/j.rinp.2017.08.009